

Line Thermodynamics: Adsorption at a Membrane Edge

P.-H. Puech, N. Borghi, E. Karatekin, and F. Brochard-Wyart*

Laboratoire PCC/UMR 168, Institut Curie, 11 rue P. & M. Curie, 75005 Paris, France

(Received 18 October 2002; published 28 March 2003)

We report a novel experimental study of line thermodynamics. Our system consists of detergent molecules adsorbing at the edges of freestanding lipid bilayers. Adsorption reduces the line tension \mathcal{T} of the membrane edges. Measuring \mathcal{T} as a function of the bulk detergent concentration C , we obtain a line adsorption isotherm. Using an extension of Gibbs's surface thermodynamics to lines, we estimate the "line excess density" of adsorbants and the energy of adsorption per site.

DOI: 10.1103/PhysRevLett.90.128304

PACS numbers: 82.70.Uv, 01.55.+b, 05.70.Np, 87.16.Dg

Introduction.—Surface thermodynamics have been extensively studied since the pioneering work of Gibbs [1]. However, the one-dimensional (1D) analog, i.e., line thermodynamics, has received very little attention, due to the lack of a suitable experimental system. In this Letter we report such a system, consisting of detergent molecules, soluble in water, adsorbing at the edges of freestanding lipid bilayers. Water *insoluble* amphiphilic molecules, such as cholesterol [2] or lysolipids [3], have an entirely different action on line energies, and are not discussed here. Only a handful of other experimental examples exist which can be considered as adsorption at a 1D substrate, such as adsorption at step edges on crystal surfaces [4], or on the grooves of carbon nanotube bundles [5]. However, contrary to our system, line energies cannot be measured directly in these examples.

A classical experimental system for studying surface thermodynamics consists of adsorption of surfactants at the air/water interface. Surfactants lower the surface tension, γ , by forming a layer at the interface [6]. Their surface density, hence the value of γ , depends on the bulk concentration, C , of surfactant in water. A typical sketch of γ vs C for such a system is shown in Fig. 1. At the lowest concentrations, surfactants are solubilized and a fraction of them adsorbs at the interface. Increasing C , γ decreases until one reaches the "critical micellar concentration" (CMC). Any further increase in C does not affect γ ; excess surfactant goes into forming micellar aggregates in the bulk. Classical surface thermodynamics relates the "surface excess," i.e., the surface concentration of adsorbants, Γ_S , to γ and C , thanks to the Gibbs's adsorption equation which, in the dilute regime, is given by

$$\Gamma_S = -d\gamma/d\mu = -(kT)^{-1}(d\gamma/d\ln C), \quad (1)$$

where $\mu \simeq kT \ln C$ is the solute chemical potential.

The 1D counterpart of this adsorption phenomenon, namely, the thermodynamics of lines, has received only some theoretical attention [7]. In 1D systems, the equivalent of the surface tension is the line tension, \mathcal{T} , and the Gibbs's relation becomes

$$\Gamma_L = -d\mathcal{T}/d\mu = -(kT)^{-1}(d\mathcal{T}/d\ln C), \quad (2)$$

where Γ_L is the "line excess" density of adsorbants. Thus, in a suitable experimental system, measurement of \mathcal{T} as a function of the bulk surfactant concentration C should allow the evaluation of the line excess.

In the present study, detergent molecules dissolved in an aqueous medium adsorb onto a "line" made up of the edges of lipid bilayers. The main challenge here is to create a long-lived and long enough "line," because lipid membranes do not like having edges. That is why they tend to form spherical or other closed forms devoid of edges. Generally, when a hole is opened in a fluid membrane, e.g., by electroporation [8], it reseals rapidly without ever growing to an optically observable size.

We have developed [9] a method to generate long-lived, micron-sized pores in membranes of giant unilamellar vesicles (GUVs), having 10–100 μm diameters. In this method, a GUV is stretched by strong optical illumination in a viscous medium. When the membrane tension of the vesicle becomes sufficiently large, a pore suddenly appears. Reaching a diameter up to $\sim 10 \mu\text{m}$, the pore closes slowly thereafter, thanks to the line tension, \mathcal{T} . Following the closure step in real time using optical microscopy allows us to extract the line tension [9]. In this system, the membrane edge is very long ($\sim 1\text{--}10 \mu\text{m}$) as compared to the thickness of the membrane ($\sim 4 \text{ nm}$) which is of molecular dimensions, such that the pore's border can be safely regarded as a line.

Using this system, we have obtained the first line adsorption isotherm, using a detergent, Tween 20, which preferentially adsorbs at the lipid membrane edges,

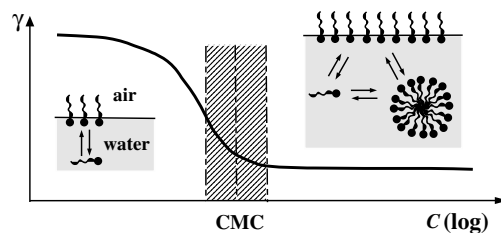


FIG. 1. Schematic plot of surface tension, γ , as a function of the bulk surfactant concentration, C , for an air/water system.

thereby reducing \mathcal{T} . From the isotherm we have estimated the line excess density of adsorbants, Γ_L , and the energy of adsorption per site.

Materials and methods.—GUVs are obtained using the “electroformation” method [10]. The lipid, 1,2-dioleoyl-*sn*-glycero-3-phosphocholine (DOPC, Avanti Polar Lipids Inc., Alabaster, AL) is cast onto conducting glass plates from organic solvent. Following evaporation of solvent, the lipid film is swollen in an aqueous buffer containing 66% v/v glycerol ($\eta_0 = 32.1 \pm 0.4$ cP) and 0.1 M sucrose under an ac field of 1.2 V at 10 Hz. At the end of ~ 6 h, 10–100 μm diameter vesicles are obtained. The membranes, which are in the L_α fluid phase at room temperature, are labeled with a fluorescent dye, N-(4-sulfobutyl)-4-(4-(diethylamino) styryl) pyridinium (kindly provided by Blanchard-Desce, Université de Rennes, France). This lipophilic dye is spontaneously inserted into the membrane, allowing observation using fluorescence microscopy (Reichert-Jung MET, Vienna, $\lambda_{\text{ex}} = 455\text{--}490$ nm, $\lambda_{\text{em}} = 580$ nm). Images captured with a CCD camera are digitized for subsequent analysis using Scion Image software. Further details on sample preparation and instrumentation can be found in Ref. [9].

Prior to observation, GUVs are resuspended in a 66% v/v glycerol, 0.1M glucose solution containing a preset concentration of Tween 20, which is a neutral surfactant with a polyoxoethylene sorbitan head and a monolaurate tail. Its hydrophilic/lipophilic balance is 16.7, classifying it as a detergent and a solubilization agent. Tween 20 can be modeled as a cone shaped molecule having positive spontaneous curvature. We have measured its CMC to be 6×10^{-2} mM in pure water and ≈ 1.2 mM in 66% glycerol solutions, using the pyrene fluorescence method [11]. This important shift of the CMC is consistent with the fact that glycerol is a less polar medium than water. The data reported here have been obtained at Tween 20 concentrations ≤ 1.2 mM, i.e., the CMC under our experimental conditions.

Pore dynamics: Line tension.—A typical sequence leading to pore opening is shown in Fig. 2. Optical illumination tensed this vesicle within ≈ 30 min [Figs. 2(a) and 2(b)]. Further illumination made a pore appear suddenly [Fig. 2(c)]. The radii of the pore and the vesicle as a function of time, measured from a sequence of images, are plotted in Fig. 3(a).

Actually, after the appearance of the first pore, numerous pores occur in succession at regular intervals of a few minutes, on the same vesicle, yet two pores never open simultaneously. Pores can appear anywhere in a vesicle; however, those appearing at the equator, such as the one shown in Fig. 2(c), are more easily amenable to image analysis [9].

Dynamics of a pore of radius r are described by [2,9]

$$4\pi\eta_s\dot{r} = 2\pi(r\sigma - \mathcal{T}). \quad (3)$$

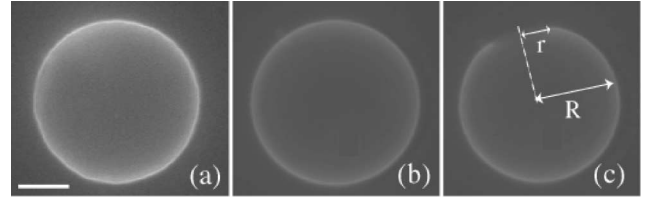


FIG. 2. Appearance of a pore in a GUV observed with fluorescence microscopy. (a) A fluctuating vesicle is illuminated with the microscope’s lamp (bar = 10 μm). (b) Within ≈ 30 min the vesicle in (a) becomes tense and perfectly spherical. (c) Further buildup of membrane tension under illumination, causes a pore to open suddenly.

The driving force for pore opening is the membrane tension, σ , while that for closure is the line tension, \mathcal{T} . Energy is dissipated in the membrane, which has a surface viscosity η_s . This is analogous to the opening of holes in viscous bare films [12], wherein σ remains constant and \mathcal{T} is neglected due to its very small value. However, pores in vesicles are more complex since σ relaxes due to two mechanisms: (i) the opening of the pore and (ii) the leakout of the internal liquid through it (caused by the excess Laplace pressure); both allow the same amount of lipid to be distributed over a smaller projected area. The membrane tension is thus a function of the pore (r) and the vesicle (R) radii:

$$\frac{\sigma(r, R)}{\sigma_0} = 1 - \frac{r^2}{r_c^2} - \frac{R_i^2 - R^2}{R_i^2 - R_0^2}. \quad (4)$$

In Eq. (4) R_i is the vesicle’s initial radius, R_0 its radius under zero tension, and σ_0 the initial membrane tension. The critical pore radius, $r_c = 2\sqrt{R_i^2 - R_0^2}$, corresponds to the complete relaxation of σ in the absence of leak out. Mechanisms (i) and (ii) are accounted for by the second and the third terms in Eq. (4), respectively. Since the product σr may become very small in (3), \mathcal{T} cannot be neglected here, unlike in the bursting of viscous bare films. In Eq. (4), R drops with the opening of a pore. Its dynamics are obtained by considering the flux, Q , of liquid passing through the pore:

$$Q = -4\pi R^2 \dot{R} = (2\sigma r^3)/(3\eta_0 R). \quad (5)$$

Equation (5) is valid as long as r varies slowly compared to the leakout velocity of the liquid. Equations (3)–(5) describe the entire life of a pore [9].

With the viscous mixtures employed in our experiments, the leakout of the inner liquid is very slow and so is the pore closure, as seen in Fig. 3(a). We focus here on this regime only, in which a measurement of the closure velocity yields \mathcal{T} , as follows. Since r varies very slowly, we make the quasistatic approximation $\sigma r - \mathcal{T} \approx 0$, from Eq. (3). Equally slowly varying is σ ; hence, we approximate $\dot{\sigma} \approx 0$ and obtain $4RR\dot{R} - r\dot{r} \approx 0$, from Eq. (4). With these approximations, we obtain

$$\dot{r} = (-2\mathcal{T}r)/(3\pi\eta_0 R^2), \quad (6)$$

using Eq. (5). What is remarkable about Eq. (6) is that the closure velocity depends only on \mathcal{T} and measurable or known parameters. After integration of Eq. (6) with the experimentally justified approximation $R \approx \text{const}$ [see inset of Fig. 3(a)], we see that a plot of $R^2 \ln r$ vs t should be linear with slope $= -2\mathcal{T}/(3\pi\eta_0)$, from which \mathcal{T} is readily obtained. As an example, the data in Fig. 3(a) is replotted in this form in Fig. 3(b). A least squares fit to the straight line portion of this plot yields a line tension of 6.7 pN in the presence of 4.9×10^{-2} mM Tween 20.

Line adsorption isotherm.—The model we have just described has previously been shown to hold for pores in bare DOPC vesicles, devoid of any detergent [9]. What happens when detergent is added? For detergent concentrations, C , up to the CMC, we have found no fundamental modification of the pore dynamics. Plots of $R^2 \ln r$ vs t yield straight lines in the slow closure regime, but with decreasing slopes (hence decreasing \mathcal{T}) as the bulk concentration of detergent is increased. For $C \approx \text{CMC}$, however, dynamics are more complicated; typically, once a pore opens it never completely reseals until all the contents of the vesicle are discharged. During this slow process, which may last up to 30 min, the vesicle membrane slowly disappears.

Measurements of \mathcal{T} as a function of C are shown in Fig. 4, up to $C \approx \text{CMC}$. For each concentration, measurements were performed on successive pores on the same vesicle, or on pores occurring in different vesicles under the same experimental conditions. No systematic variation of \mathcal{T} was found in measurements made on successive

pores, over the time scale of an experiment (typically 3 h). Moreover, the scattering of measurements on successive pores is as important as that observed between different vesicles. Finally, there is ample time for establishing equilibrium between the bulk and the line during the lifetime of a pore (1–100 s), assuming that the time scales for exchanging a detergent molecule between the bulk and the line are comparable to typical lifetimes of a detergent in a micelle (10^{-5} – 10^{-3} s [6]).

Looking at the isotherm in Fig. 4, we identify three distinct regimes. For the lowest concentrations of Tween 20, the line tension decreases as more detergent is added (regime I). This continues up to a concentration $C = C^* \approx 10^{-2}$ mM, beyond which \mathcal{T} reaches a plateau (regime II, $C^* < C < C^{**} \approx 5 \times 10^{-2}$ mM). There exists a third regime for $C > C^{**}$, in which \mathcal{T} decreases again with increasing C .

The first two regimes in the isotherm of Fig. 4(a) are analogous to a classical surface adsorption isotherm for a soluble surfactant (cf. Fig. 1). In regime I detergent is partitioned between bulk solution and the edges of a pore, as drawn schematically in Fig. 5(a). The preference of the detergent for the pore's line is due to its conical shape with a large hydrophilic head. It can thus significantly reduce the edge energy of a membrane by adsorbing at the borders. As the bulk detergent concentration is increased, the border becomes saturated with detergent at $C \approx C^*$. Any further detergent added into the system must go into a reservoir. Micelles are excluded as a reservoir, since we are well below the CMC. Instead, we expect that excess detergent goes into the lipid membrane in regime II [Fig. 5(b)]. For these two regimes, a plot of \mathcal{T} vs $\ln C$ [Fig. 4(b)] allows us to estimate the line excess, Γ_L , at

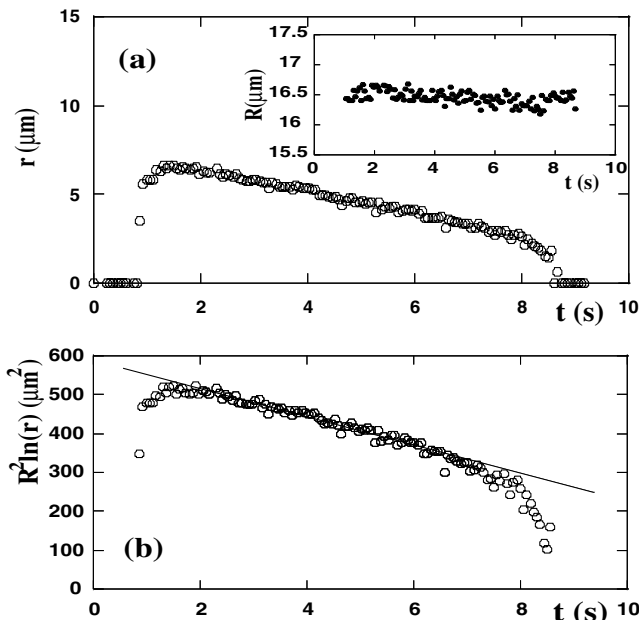


FIG. 3. (a) Pore (r , \circ) and vesicle radii (R , \bullet , inset) as a function of time for a DOPC vesicle in the presence of 4.9×10^{-2} mM Tween 20. (b) $R^2 \ln r$ plotted against time for the same pore. The least squares fit to the linear part has slope $\approx -44.7 \mu\text{m}^2/\text{s}$, which implies $\mathcal{T} \approx 6.7$ pN (see text).

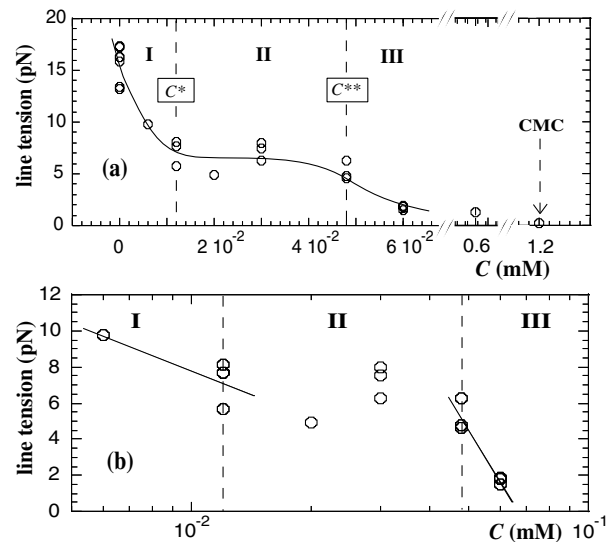


FIG. 4. (a) Line tension of DOPC membrane edges as a function of bulk Tween 20 concentration, C . (b) The data in (a) (except for $C = 0$ and the two highest concentrations) plotted on semilogarithmic coordinates. The linear fit in regime I has slope ≈ -9 pN, while that in regime III has slope ≈ -40 pN.

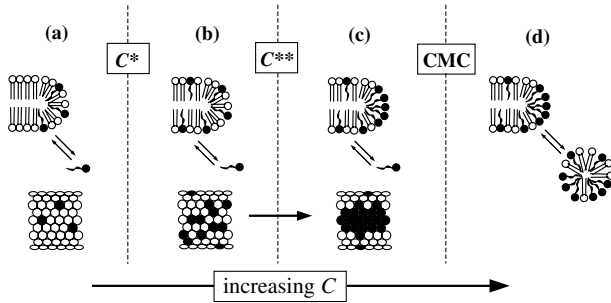


FIG. 5. Proposed interactions between the pore's edge and detergents in different regimes. Top row: transversal view. Bottom row: front view of the membrane edge, with dark (white) dots representing detergent (lipid) headgroups.

$C \approx C^*$. The straight line fitted to the data in regime I in Fig. 4(b) has slope ≈ -9 pN, implying $\Gamma_L \approx 2 \text{ nm}^{-1}$, from Eq. (2). This is a reasonable value, assuming that the detergent head group occupies an area similar to that of the lipid ($\approx 60 \text{ \AA}^2$), and considering that the line can, in fact, accommodate a few molecules along its thickness, as drawn schematically in Fig. 5.

Increasing the bulk detergent concentration above C^{**} we reach regime III, in which the line tension starts decreasing again. This is an indication of a new organization in the system. In this regime, fitting a straight line to the data near C^{**} in Fig. 4(b), we find a slope ≈ -40 pN, which implies a line density of $\approx 9 \text{ nm}^{-1}$. The line can still accommodate such a high density, provided the detergent molecules are organized in a condensed manner, as shown schematically in Fig. 5(c). The sharp change of slope at C^{**} is reminiscent of a transition from a dilute to a condensed phase when a nonsoluble amphiphile is compressed at the water/air interface.

For C approaching the CMC [the two highest detergent concentrations in Fig. 4(a)], the integrity of the lipid membrane is progressively lost. At such high concentrations we typically observe a single pore which lasts until the whole vesicle is slowly dissolved, possibly via formation of lipid-detergent mixed micelles [Fig. 5(d)].

We estimate the energy of adsorption per site, ϵ , as follows. For n molecules, each of size a , adsorbed on a line of length L , the free energy per site is $(a/L) \times (F/kT) = -\phi\epsilon/(kT) + \phi \ln\phi + (1-\phi) \ln(1-\phi)$, where $\phi = na/L$ is the fraction of occupied sites. The “line osmotic pressure” is then $\Pi_L = (\partial F/\partial L)_n = -(kT/a) \times \ln(1-\phi)$. Calculating $\mu = \partial F/\partial n$ and equating it to $kT \ln(Ca^3)$ gives us $\phi/(1-\phi) = Ca^3 \exp(\epsilon/kT)$. Using this in the expression for Π_L , we write

$$\mathcal{T} = \mathcal{T}_o - \Pi_L = \mathcal{T}_o - (kT/a) \ln(1 + Ca^3 e^{\epsilon/kT}). \quad (7)$$

The reader can verify that Eq. (7) is consistent with the Gibbs relation in Eq. (2). A fit of Eq. (7) to our data in regimes I and II with $a \approx 1 \text{ nm}$ yields $\epsilon \approx 12kT$, a value comparable to measured heats of adsorption of typical detergent molecules to lipid membranes [13].

In summary, we have measured the first line adsorption isotherm. This is an essential step in understanding the interactions between lipid membranes and amphiphiles which are expected to adsorb preferentially at membrane edges. These amphiphiles, which may be called “edge-actants” [14], may be artificial, such as Tween 20, and have technological applications, or they may be natural, such as the protein talin [14] or lysolipids [3], and have crucial biological functions.

A remarkable phenomenon related to the interaction of amphiphiles with lipid bilayers is membrane fusion, which remains an enigma and a challenge in molecular biology [15]. In fact, the energy barrier to nucleate a pore in a membrane is very sensitive to \mathcal{T} : we observe spontaneous fusion events between GUVs when \mathcal{T} is sufficiently lowered in the presence of Tween 20 [16].

We thank P.-G. de Gennes, J. Prost, A. Buguin, and O. Sandre for stimulating discussions. E. K. gratefully acknowledges funding by the Fondation pour la Recherche Médicale and EMBO.

*Corresponding author: francoise.brochard@curie.fr

- [1] J.W. Gibbs, *The Collected Works of J. Williard Gibbs* (Dover, New York, 1971), Vol. 1.
- [2] E. Karatekin *et al.*, *Biophys. J.* **84**, 1734 (2003).
- [3] L.V. Chernomordik *et al.*, *Biochim. Biophys. Acta* **812**, 643 (1985).
- [4] X. Chen *et al.*, *J. Vac. Sci. Technol. B* **14**, 1136 (1996); G. A. Samorjai, *Chemistry in Two Dimensions: Surfaces* (Cornell University Press, Ithaca, 1981).
- [5] S. Talapatra and A.D. Migone, *Phys. Rev. Lett.* **87**, 206106 (2001).
- [6] J.N. Israelachvili, *Intermolecular and Surface Forces* (Academic Press, London, 1992), 2nd ed.
- [7] M. Vignes-Adler and H. Brenner, *J. Colloid Interface Sci.* **103**, 11 (1985); P. Chen, *Colloids Surf. A* **161**, 23 (2000); A.I. Rusanov, *ibid.* **156**, 315 (1999); V.G. Babak, *ibid.* **156**, 423 (1999).
- [8] *Guide to Electroporation and Electrofusion*, edited by D.C. Chang *et al.* (Academic Press, San Diego, 1992).
- [9] F. Brochard-Wyart *et al.*, *Physica (Amsterdam)* **278A**, 32 (2000); O. Sandre *et al.*, *Proc. Natl. Acad. Sci. U.S.A.* **96**, 10591 (1999).
- [10] *Giant Vesicles*, edited by P.L. Luisi and P. Walde (Wiley, New York, 1999).
- [11] G. Lantzsch *et al.*, *Langmuir* **14**, 4095 (1998).
- [12] G. Debrégeas, P. Martin, and F. Brochard-Wyart, *Phys. Rev. Lett.* **75**, 3886 (1995).
- [13] H. Heerklotz and J. Seelig, *Biochim. Biophys. Acta* **1508**, 69 (2000).
- [14] A. Saitoh *et al.*, *Proc. Natl. Acad. Sci. U.S.A.* **95**, 1026 (1998).
- [15] J. Zimmerberg, *Trends Cell Biol.* **11**, 233 (2001).
- [16] E. Karatekin, O. Sandre, and F. Brochard-Wyart, *Polym. Int.* **52**, 486 (2003).